METALS AND MATERIALS, Vol. 6, No. 1 (2000), pp. 39~49

Development of Crystallographic Texture during Processing of Some Aluminide Based Aerospace Materials

R. K. Ray and Satyam Suwas

Department of Materials and Metallurgical Engineering, Indian Institute of Technology
Kanpur-208016, INDIA

Because of their lower specific weights, remarkably high strength and improved oxidation resistance, the aluminide-based intermetallic compounds are the candidates for substituting the rather heavy superalloys, at present used in compressors and turbines of aircraft engines. The ordered intermetallic compounds based on Ni_3Al and Ti_3Al have stimulated much interest due to their attractive and somewhat unusual properties. Thermomechanical processing constitutes an important route for forming these materials into suitable shapes for various applications. The processing route also influences the texture of the product, which in turn dictates the final properties. The present work summarises the evolution of textures during thermomechanical processing involving cold / hot rolling and subsequent annealing of a two phase Ni_3Al base and a two phase Ti_3Al base alloy.

Key words : aerospace materials, aluminides, thermomechanical processing, texture, Ni_3Al, Ti_3Al

1. INTRODUCTION

With the advent of gas turbine engines in aviation in the late 1930s, the search for materials with even higher temperature capability was undertaken in right ernest. The rather successful utilisation of nickel base superalloys in both land-based and aero-gas turbines led to the commercialisation of new materials that are predominantly intermetallic in nature. Research over the last two decades on high temperature structural aerospace alloys has concentrated overwhelmingly on intermetallic alloys. For both the important engine components, compressors as well as turbines, intermetallic materials are the candidates for substituting the rather heavy superalloys, because of their lower specific weights, remarkably high strength and improved oxidation resistance. These materials have stimulated much research interest due to their attractive and somewhat unusual properties. The ordered intermetallic compounds have long range crystal structures below a critical temperature. An ordered structure in intermetallics is favoured by greater strength of bonds between unlike atoms as compared to like atoms. Among the intermetallic compounds, aluminide intermetallics have been recognised as candidates for next generation high temperature materials. This is primarily due to the benefits gained from their much lower densities as compared to the existing alloys under use. However, the technological importance of these aluminides is due basically to their excellent structural stability upto the order-disorder transformation temperatures. The transformation temperature is often quite high, sometimes the material is ordered even upto its melting point. In addition, they possess relatively high melting point, good high temperature strength and also are capable of forming a protective surface coating of alumina against further oxidation at high temperatures [1]. Although aluminides in their polycrystalline form exhibit brittle fracture and low ductility at ambient temperatures, metallurgical solutions have been found out that offer the possibility of engineering applications through modified processing techniques [2]. These include control of chemistry and microstructures. A third metallurgical variable, which is likely to dictate many of the mechanical properties and therefore has a great influence on product performance capabilities, is the crystallographic texture. In recent years a detailed investigation on the evolution of texture during processing of a number of aluminide intermetallics of Ni and Ti has been undertaken in our laboratory. The results of these investigations are enumerated below along with those from other research groups in this area.

This article is based on a presentation made in the symposium " '99 International Symposium on Textures of Materials", held at Sunchon National University, Sunchon, Korea, April 21 ~ 22, 1999 under the auspices of The Korean Institute of Metals and Materials and the Research and Development Center for Automobile Parts and Materials.

2. ALLOYS BASED ON Ni_3Al

The conventional structural aerospace materials, the nickel base superalloys, derive much of their high temperature strength from nickel aluminides and nickel silicides that comprise as much as 60 vol.% of the superalloys. Ni_3Al is the main strengthening constituent of Ni-base superalloys. When used as a monolithic material, its advantages include high temperature strength, high creep strength, high stiffness, low density and high resistance to oxidation. Owing to these properties, the applications of these intermetallics are envisaged in various aerospace components, especially in monolithic forms and as composites. Nickel aluminides based on Ni_3Al have become the subject of large scale development programmes. These were initiated by Aoki and Izumi [3], who were able to ductilise the essentially brittle γ' phase by adding small amount of boron to Ni_3Al. The yield strength of this material increases with increase in temperature upto 873 K. Such positive variation of strength with temperature is quite opposite to the behaviour of conventional metals and alloys. The substantial room temperature ductility of boron-doped Ni_3Al makes it a material suitable for processing by conventional routes, i.e. by cold forming and annealing. Such thermomechanical treatments (TMT) produce changes in microstructure as well as crystallographic texture which ultimately affect mechanical properties.

A number of multiphase Ni_3Al base alloys have been developed recently [4]. Suitable alloying additions impart attractive mechanical properties to these multiphase alloys. The two phase Ni_3Al base alloy Ni-21.8Al-0.34Zr-0.1B consists of the ordered Ni_3Al (γ') phase along with a Ni-base disordered FCC phase (γ). Such a two-phase material is expected to exhibit a better combination of strength and ductility; at the same time, the ternary additions are expected to enhance the materials properties even further. Due to the presence of Zr and the two-phase structure, the grain growth in such materials could be effectively controlled. This material has very good hot corrosion resistance also. The cold workability of this alloy is excellent due to its (γ'+γ) two-phase structure which also imparts superplasticity during forming of this alloy [5, 6, 7]. Textural evolution during cold rolling and also during subsequent annealing of this material has been studied in detail [8].

The alloy was obtained in the form of a 1mm thick continuously cast sheet. The same was homogenised at 1433 K for 24 hrs. The homogenised alloy was subjected to cold rolling reductions of 25%, 35%, 45%, 55%, 65% and 73%. A careful examination of the ODFs (Figs. 1(a)-(f)) for these rolled materials reveals the presence of a weak copper type texture comprising the components Bs{011}<211>, Cu{112}<111>, Goss{011}<100> and S{123}<634> after 25% deformation. The overall texture intensifies significantly in the case of 35% rolled material. In addition to a sharp Bs component, a prominent maxima appears a few degrees away from the Bs. The Cu and Goss components are relatively weak. In the 45% rolled material, sharpness of texture decreases with no change in the locations of the components. For the rolling reduction of 55%, the ODF is

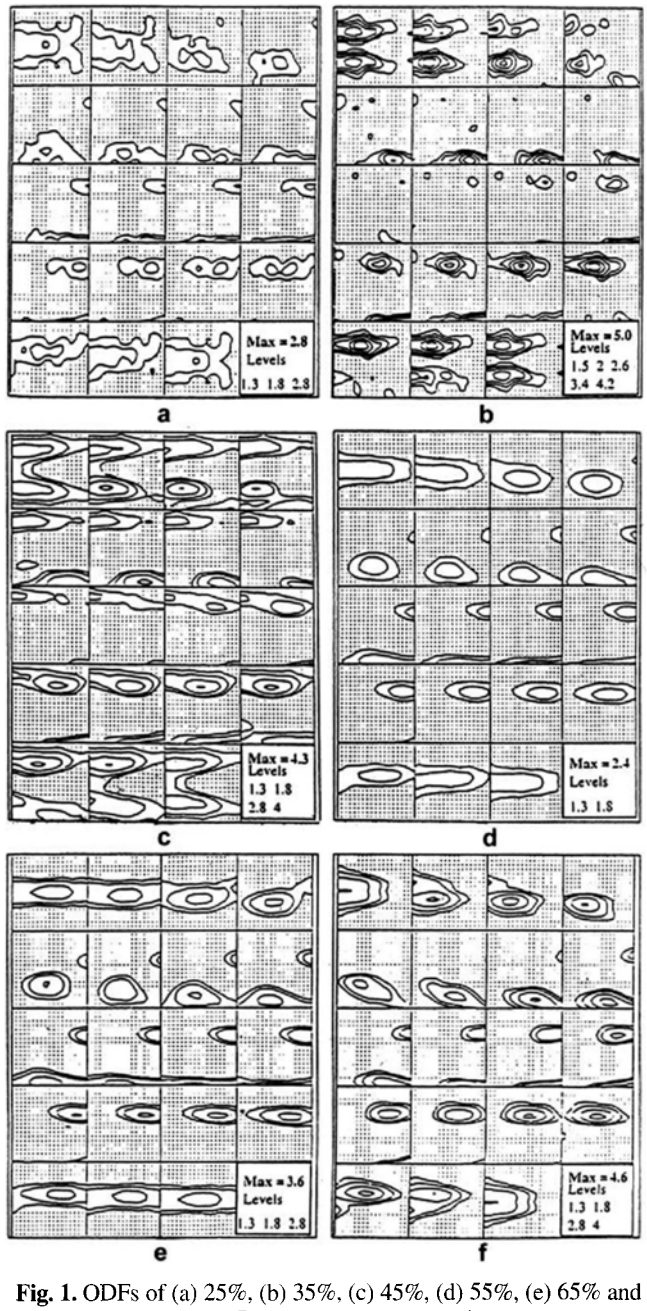

Fig. 1. ODFs of (a) 25%, (b) 35%, (c) 45%, (d) 55%, (e) 65% and (f) 73% cold rolled Ni_3Al (B, Zr) at constant ϕ_2 sections.

found to be significantly weaker, however it resembles the texture for the 25% rolled material in both nature and intensity. The overall texture sharpens with deformation beyond this stage with the Bs component becoming the most prominent one.

The examination of the various texture fibres in the ODFs of the as-rolled materials reveals that a well developed β-fibre (Fig. 2) forms after 35% deformation, which does not change much after 45% deformation. The intensity of this fibre decreases drastically after 55% rolling reduction. The fibre intensity, however, improves again after 65% reduction and strengthens considerably at a deformation level of 73%. The maximum value of the β-fibre occurs at a location between Bs and S, which is known as the Bs/S position {168}<211>. The unusually high β-fibre intensity after 35% deformation, with the highest intensity near the Bs/S {168}<211> and a substantially high intensity at the Bs location, resembles the characteristics of alloy type texture. Evidence of twinning has been found in the microstructure at this stage (Fig. 3(a)). Therefore, the changeover from pure metal to alloy type has probably been brought about by twinning. Extensive twinning has also been reported for a pure γ' alloy Ni_3Al(B) [9] for 65% rolling deformation and this also brought about a similar texture transition. The formation of twins after cold deformation in both the alloys has been attributed to a structural transformation in the γ' phase from $L1_2$ to DO_{22} [10]. The high intensity of the S component of the β-fibre (more specifically the Bs/S component, {168}<211>) after 35% deformation appears rather unusual. Although the Cu component of the β-fibre is known to reduce substantially due to twinning, Hirsch *et al.* [11] suggested that the orientation (123)[$\bar{4}\,\bar{1}$2] near S produces its symmetrically equivalent variant (123)[41$\bar{2}$] after twinning. Thus the intensity of S component is supposed to be unaffected by twinning. Although the deformation of the γ regions is also expected to contribute both to the Cu and S components during deformation, their magnitudes will be rather small and therefore cannot account for the high intensity of the β-fibre at Bs/S location. After 45% cold work, a few shear bands are seen in the microstructure (Fig. 3(b)) in addition to a high density of twins. The shear bands are broad (Fig. 3(c)), and extend over many grains indicating that these could be of Bs type [11]. The crystallites present within these shear bands will therefore have certain preference for the Goss {011}<100> orientation [12] and this may be the reason for the sharpening of this component after 45% deformation. The density of microbands has been found to increase continuously with rolling reduction accounting for the rapid sharpening of the Goss component till the final 73% rolling reduction. A typical microstructure showing twins in 73% rolled material is shown in Fig. 3(d).

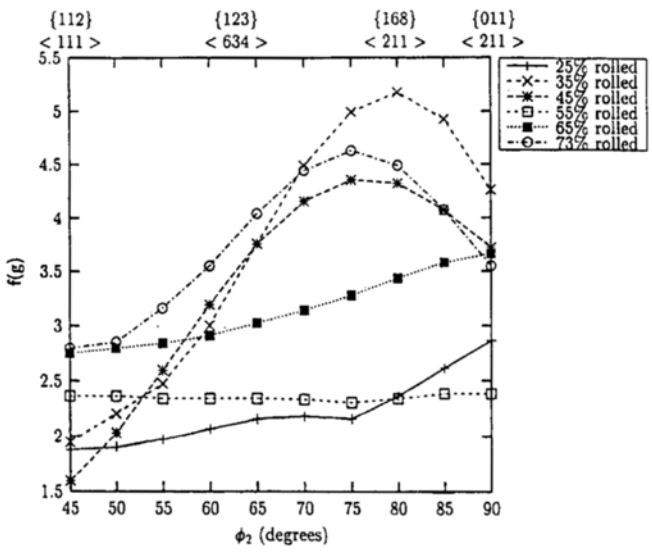

Fig. 2. β-fibre plots for 25%, 35%, 45%, 55%, 65% and 73% cold rolled Ni_3Al (B, Zr).

The α-fibre plot (Fig. 4) for the 25% rolled material indicates the presence of the Goss {011}<100> component and the peak appears near about the Bs/Goss {011}<511> position. After 35% rolling, the Goss component weakens significantly and after 45% rolling this reappears and gradually intensifies till 73% rolling reduction. The rotated Goss {011}<011> component is reasonably sharp after 65% rolling but then it drastically weakens after 73% reduction. The {011}<111> component emerges as the most prominent one for the 45% as well as the 65% rolled specimens whereas for the 73% rolled material the maxima appears somewhere in between Bs/Goss and Bs location. The τ-fibre plots for all the cold rolled materials (Fig. 5) show that the orientation maxima in each case is located at the Cu and the Goss position.

Very limited work has been carried out on the deformation texture of $L1_2$ ordered materials like Ni_3Al. Hutchinson *et al.* [13] were the first to study the texture evolution in a similar alloy, such as the Cu_3Au, in the ordered and the disordered states. Gottstein and co-workers have studied the evolution of deformation and recrystallisation textures in Ni_3Al(B) and its other modified versions [14-19]. They [14] found that the rolling texture of boron doped Ni_3Al mainly consists of the Bs {011}<211> and Goss {011}<100> components. This is contrary to the expectation that the texture should be of pure metal type, as the stacking fault energy of Ni_3Al (~130 mJ/m^2) is comparable with that of pure Ni (~150 mJ/m^2). The origin of

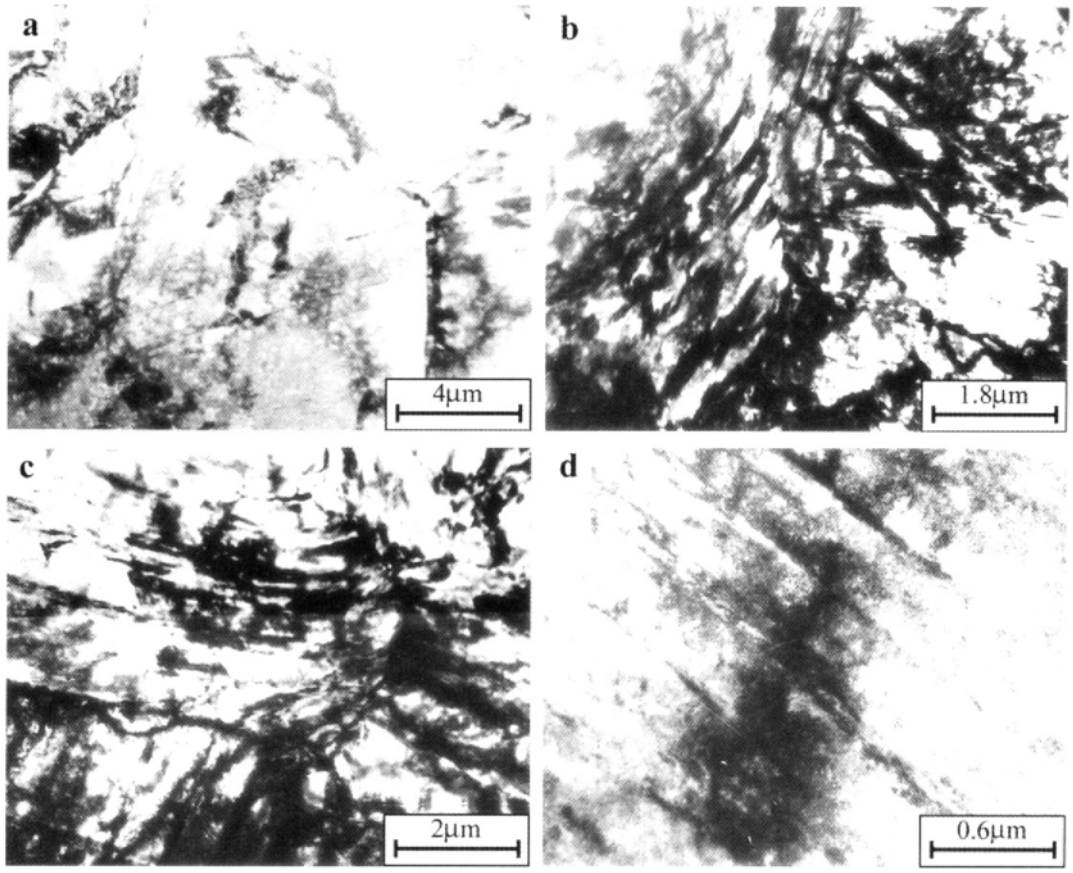

Fig. 3. TEM micrographs of $Ni_3Al(B, Zr)$ for (a) 35% cold rolled condition showing the evidence of twins, (b) 45% cold rolled condition showing shear bands, (c) 45% cold rolled condition showing microbands and (d) 73% cold rolled condition showing twins.

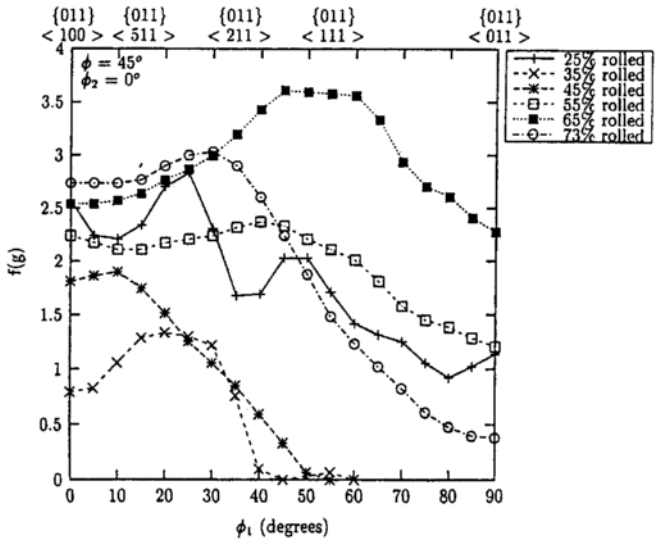

Fig. 4. α-fibre plots for 25%, 35%, 45%, 55%, 65% and 73% cold rolled Ni_3Al (B, Zr).

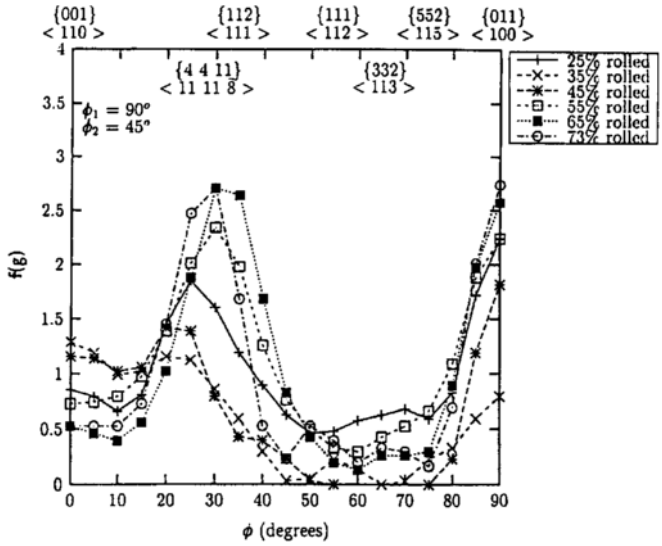

Fig. 5. τ-fibre plots for 25%, 35%, 45%, 55%, 65% and 73% cold rolled Ni_3Al (B, Zr).

this α-brass type texture has been attributed to the formation of shear bands generated by the heavy deformation. Ball and Gottstein [15] from their TEM investigation have shown the presence of profuse microband clusters and shear bands on the longitudinal section of a 70% cold rolled $Ni_3Al(B)$ sample.

Texture transformation of the above type (from pure metal to alloy) has been predicted by Wassermann [20] to occur when mechanical twinning is also available as a deformation mode in addition to normal slip. Later work by Duggan *et al.* [12] suggested that during continued cold rolling, other homogeneous modes of deformation may be inhibited and localised shear bands will form. Due to the inability of the material to sustain further work hardening, the near Cu orientations are expected to become unstable and there also may by a rotation of {011}<100> by shear banding. Further deformation within the substructure will then lead to brass texture formation. Electron microscopic studies revealed a transition in deformation mode from slip to twinning, at the same strain level. The texture transformation has been explained in terms of a structural transformation from $L1_2$ to DO_{22} during cold rolling [10, 21, 22]. Continued deformation of the DO_{22} structure leads to more twin formation, which changes the texture from pure metal type to alloy type.

In order to study the evolution of annealing texture in this alloy, the 73% rolled material was annealed at 1173 K for different lengths of time. The pole figures of all the annealed samples look quite similar and all of them signify a rather weak texture. A study of the ODF plots (Fig. 6) shows the presence of a strong Bs component along with a Goss component after 4 minutes of annealing. These components weaken after 10 minutes of annealing. A rotated Goss component with an orientation very near to {011}<111> appears after 1 hr, which also weakens after 3 hrs. Another component {123}<121>, which is basically a rotated variation of the S component {123}<634>, developes at the final stage.

The β fibre plots (Fig. 7) for the annealed materials show that both Cu and Bs components decrease at the very initial stages, and a situation close to the equilibrium is achieved after 1 hr of annealing, beyond which the overall texture does not change. It is also observed that the intensity of the Cu component decreases more rapidly as compared to that of the Bs component. The intensity of the former becomes quite low after 4 minutes of annealing while the Bs component is not totally suppressed even after 1 hr of annealing.

As reported in case of pure Ni_3Al(B) [9], in this alloy also a drastic weakening of deformation texture occurs during the recovery stage and this has been found to be associated with the restoration of the initial $L1_2$ structure from the DO_{22} of the heavily deformed γ′ phase [8]. A typical micrograph showing the recovery stage is shown in Fig. 8 (a). Thus the texture at the beginning of the recrystallisation process is already weak and it remains so till the

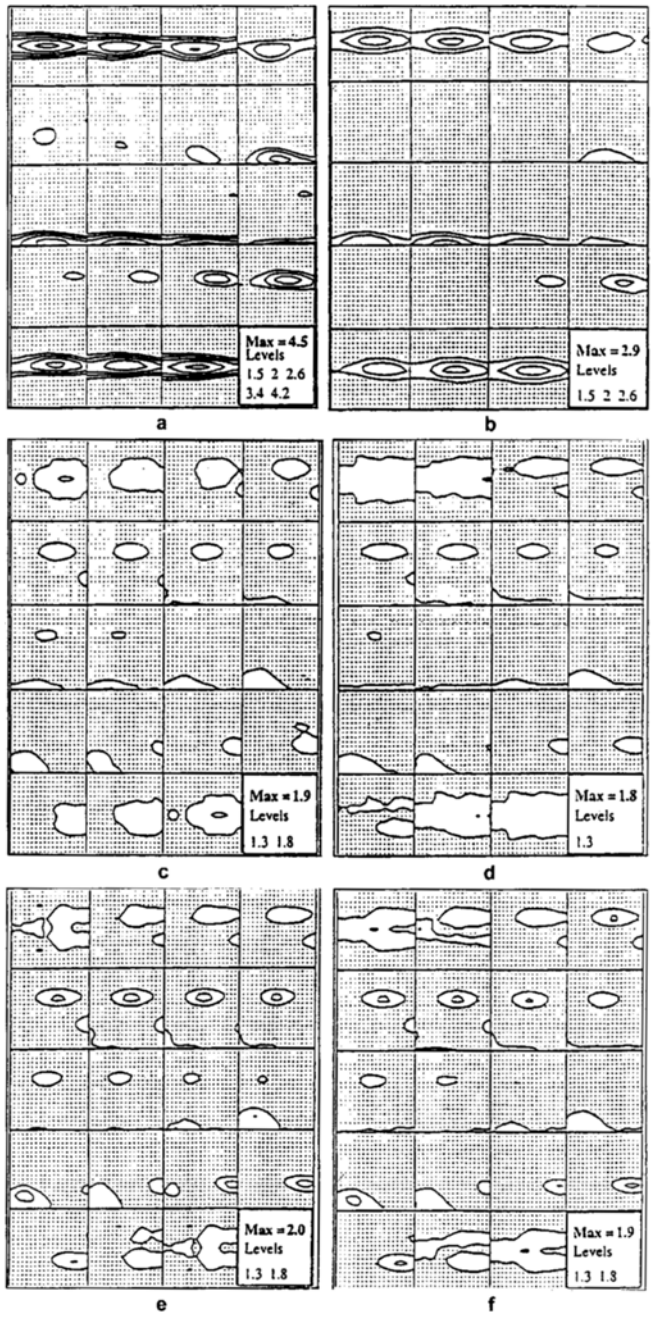

Fig. 6. ODFs of Ni_3Al (B, Zr) after annealing at 1173 K for (a) 4 min, (b) 10 min, (c) 1 hr, (d) 10 hrs, (e) 12 hrs and (f) 15 hrs.

process of recrystallisation is complete. A high density of randomly oriented nuclei seems to contribute towards this phenomenon. The first recrystallised nuclei appear in the disordered γ regions within the shear bands. With the progress of recrystallisation numerous such grains will appear which will lack any growth selection and hence the overall texture is weak. A cluster of recrystallised grains is shown in Fig. 8 (b). After recrystallisation of the deformed γ phase is complete, the deformed γ′ phase starts recrys-

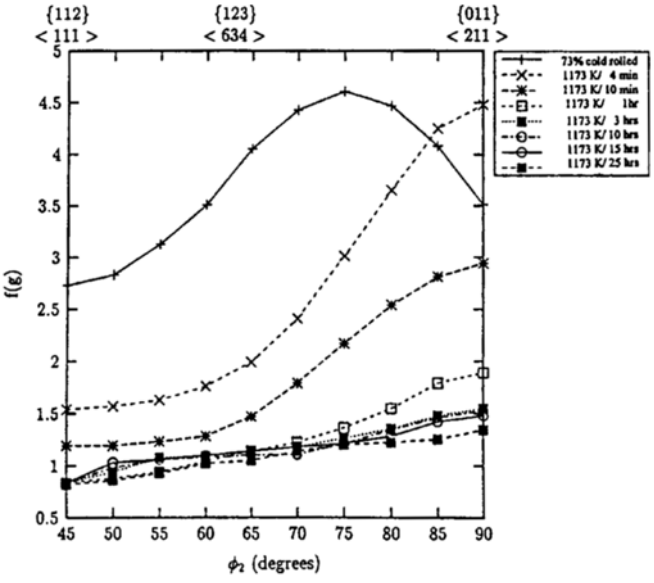

Fig. 7. β-fibre plots for Ni_3Al (B, Zr) after annealing at 1173 K for different time intervals.

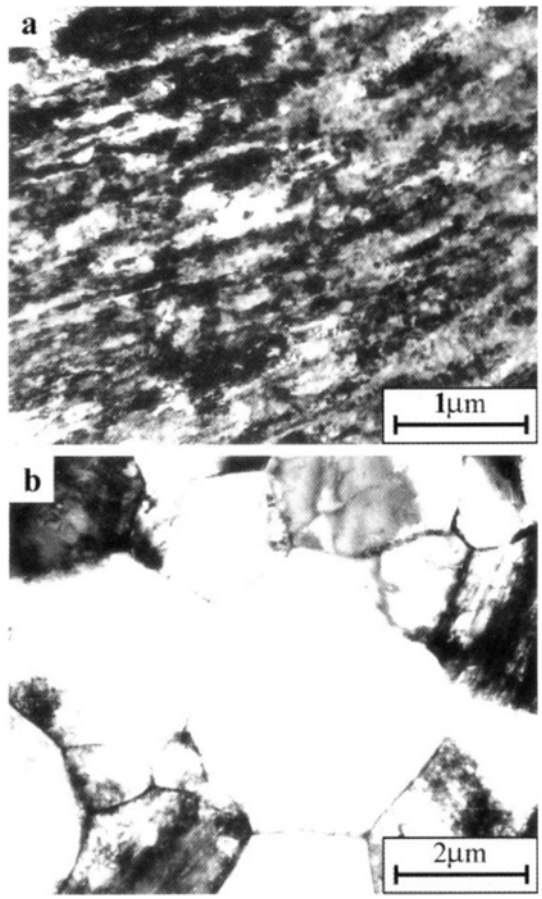

Fig. 8. TEM micrograph of Ni_3Al(B, Zr) after annealing showing (a) partly recovered area and (b) a cluster of recrystallised grains.

tallising. The final texture is not much different from random, indicating that the material will be nearly isotropic at the end of the deformation and recrystallisation processing.

Earlier works on the recrystallisation texture evolution in Ni_3Al(B) by Gottstein *et al.* [18] also revealed a rather weak annealing texture with the components {310}<135> and {211}<135> (at 923 K) and only {310}<135> at 973 K. The evolution of weak recrystallisation texture in Ni_3Al(B) has also been observed by Ghosh Chowdhury *et al.* [9]. In a subsequent study, Gottstein and co-workers [19] as well as Ghosh Chowdhury *et al.* [9, 23] observed very weak recrystallisation texture consisting of the components {025}<100> (rotated cube) and {011}<100> (Goss) in the same alloy. In the two phase alloy Ni_3Al(B, Zr, Fe), Ball *et al.* [16] observed the S {123}<634> orientation along with weak rotated cube components.

3. ALLOYS BASED ON Ti_3Al

Conventional high temperature Ti-base alloys have reached an operating temperature close to 873 K, which has essentially been determined by their creep and oxidation resistance. The need for advanced aerospace materials arose primarily for use at higher service temperatures and also to satisfy the requirements for higher specific strength at the same time. The materials most suited to these demanding needs are the alloys based on titanium aluminides [24]. The alloy system based on the compound Ti_3Al is among the oldest in this series. Large research efforts were directed towards the developments of these aluminides, which took care of the methods of improving ductilisation as well as enhancing the strength. The room temperature equilibrium phase of Ti_3Al is referred to as the hexagonal α_2 phase (DO_{19}). Due to its crystal geometry and ordered structure, it has poor room temperature ductility. In spite of these limitations, a number of components in the compressor and turbine sections of the aero-engine have already been successfully fabricated from titanium aluminides and attempts are underway to improve their low ductility and poor toughness at lower temperature, so that their application-base is further extended. Nb addition has been proven to be the most effective for increasing the inherent low temperature ductility of binary Ti_3Al [25]. It achieves this by increasing the number of active slip systems and enhancing the occurrence of cross slip [26]. The equilibration of high temperature b.c.c. β phase is also instrumental in increasing ductility by relieving the strain incompatibilities at α_2 interfaces [26]; in addition it also increases the fracture toughness of these alloys. The first reference alloy developed in this connection is the one with

nominal composition Ti-24Al-11Nb (in at %). Strengthening of Ti_3Al alloys is most readily controlled through thermomechanical processing (TMP). The proper combination of working and heat treatment can increase the strength of a particular alloy by more than 50%, which is much higher than what can be accomplished through minor alloying changes [24, 27]. An increase in strength can also be brought about through the refinement of the microstructure. The applications of these alloys in the aerospace industry are typically in the manufacture of honeycomb structures for fuselage panels for advanced aerospace designs, noise damping components in modern jet turbines, turbine nozzle guide vanes etc. In addition, Ti_3Al-base alloys also find application as laminated composites. Such applications would require titanium aluminide to be processed into thin sheets and foils. However, alloys having low ductility are generally not amenable to cold rolling. It is, therefore, recommended to process them by hot/warm rolling and annealing route. Further, the phase fractions and other microstructural attributes can be controlled by proper heat treatments. The sheet processing methods are also expected to have pronounced effect on the development of texture in these materials. Since texture is known to affect the mechanical properties very significantly, investigations into these aspects are also of utmost importance. Mechanical processing of materials with h.c.p. structure causes the development of strong texture as well as the refinement in the grain size, and both these changes influence the mechanical properties of the product. The processing parameters that affect the texture development in a rolled material are mainly the temperature of processing and the amount of rolling deformation. Although the production of Ti_3Al-base alloys (Ti-24Al-11Nb in particular) into sheet form has long been attempted, very little attention has been paid till date to elucidate the evolution of texture in these materials. A research programme was therefore undertaken to carry out a systematic study of the evolution of texture during thermomechanical processing of the Nb containing Ti_3Al-base alloy Ti-24Al-11Nb [31].

Whatever scanty information is available on the development of texture in Ti_3Al base alloys, particularly in Ti-24Al-11Nb or an alloy close to this stoichiometry during hot rolling is in the form of mostly pole figures only [28, 29]. The most comprehensive amongst these is due to Hon *et al.* [28], which aimed at examining the evolution of hot rolling texture in a $Ti_{65}Al_{25}Nb_{10}$ alloy. It has been reported that using a proper rolling process involving unidirectional multipass rolling at 1153 K, a basal texture could be developed in this material. It was also inferred from this investigation that a lower temperature of rolling and a higher degree of rolling deformation could be favouring the evolution of basal (0002) α_2 texture with improved intensity. Rolling at higher temperatures, where the content of β phase is more, could impose additional constraints on the rotation of α_2 grains, thereby lowering the intensity of (0002) α_2. All evidences from the work by Hon *et al.* point to the fact that the sharp basal texture in the $Ti_{65}Al_{25}Nb_{10}$ alloy is caused by the deformation of the α_2 grains during the rolling process.

The experimental procedure, in the investigation on Ti-24Al-11Nb alloy carried out in our laboratory [31], consisted of hot rolling of the as-cast alloy, in the temperature range 1173 K-1523 K to a maximum deformation of 80%, followed by either water quenching or furnace cooling from the respective rolling temperatures. Some pieces of the as-cast material were given a prior heat treatment for the equilibration of phases and then subjected to rolling at 1173 K by different amounts of reduction (50%-80%), again followed by water quenching. Some of the hot rolled materials were subjected to isochronal annealing for 1 hr within the temperature range 1123 K-1293 K (at ~50 K intervals) and also to isothermal annealing at 1173 K for different time intervals (1 hr-12 hrs).

The results of the investigation indicate that when the starting material is rolled at 1173 K, basal texture is obtained, both in the water quenched and in furnace cooled conditions. Among these two the former gives rise to a sharper basal texture. The texture maxima are mainly located along the fibre [0001] || ND (~12° from the exact location along RD), and a few strong intensity peaks are also observed at $[10\bar{1}0]$ || RD (Fig. 9(a)). Rolling at a temperature of 1293K, which is ~80K below the β-transus results in a weak basal texture (Fig. 9(b)).

In order to have an idea about the texture formation in α_2 obtained from β by transformation, hot rolling at temperatures above the β-transus followed by water quenching and furnace cooling were carried out. Two temperatures were chosen for this purpose, namely, 1373 K which is just near the $\alpha_2+\beta/\beta$ phase boundary, where there is only a feeble chance of β recrystallisation, and 1523 K where the β phase is likely to get an opportunity to recrystallise before transformation. The β rolling textures in both the cases are more or less similar, with {011}<uvw>, {112}<uvw>, {113}<uvw> and {223}<uvw> as the main components along with several other weaker components. The textures of the transformed α_2 obtained upon furnace cooling from the two temperatures are, however, different in the two cases (Fig. 10). In the materials rolled at 1373 K and furnace cooled, the texture formed in transformed α_2 is completely non basal (Fig. 10(a)). On the other hand, furnace

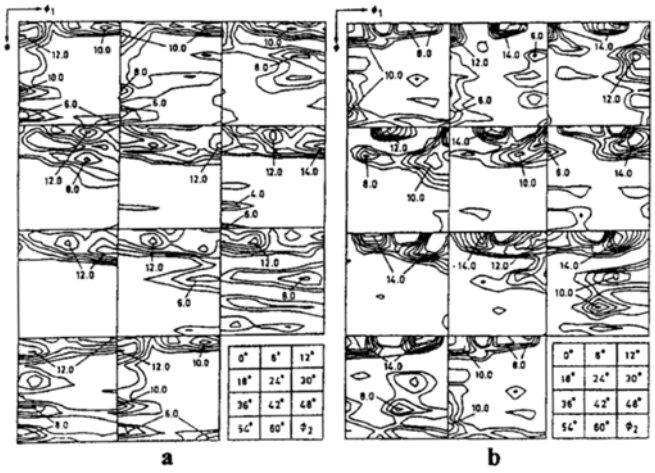

Fig. 9. ODFs for the alloy Ti-24Al-11Nb for as-cast material rolled to 80% reduction at (a) 1173 K and (b) 1293 K (water quenched).

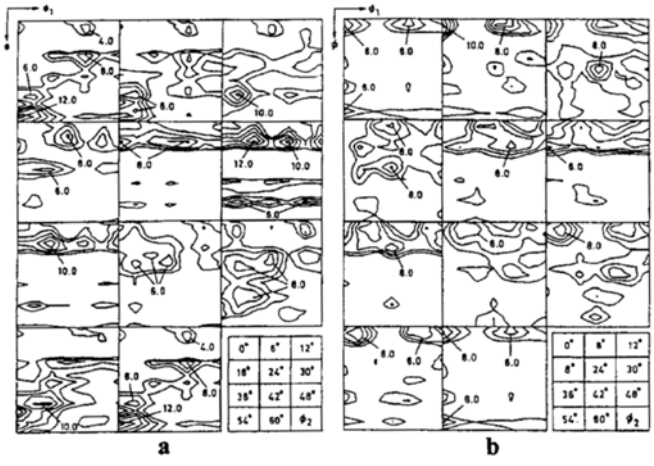

Fig. 10. ODFs of the Ti-24Al-11Nb alloy rolled to 80% reduction at (a) 1373 K and (b) 1523 K (furnace cooled).

cooling of the material rolled at 1523 K gives rise to a basal texture (Fig. 10(b)). This difference in texture has been attributed to the differences in variant selection during $\beta \rightarrow \alpha_2$ transformation in the above two cases [31]. TEM study reveals that when rolled at 1373 K the material remains in the deformed β state, whereas the β phase becomes strain free in the material rolled at 1523 K (Figs. 11(a) and (b)).

The material, which was prior heat treated at 1173 K for a long time before rolling again at 1173 K upto 80% reduction, exhibits an even sharper basal texture as compared to the samples mentioned above. In this case, most of the orientations are concentrated along the [0001] || ND fibre. The degree of deformation during rolling also has a profound effect on the nature and extent of texturing. The material rolled at 80% reduction at 1173 K shows a sharper basal texture than the one rolled to 50% reduction

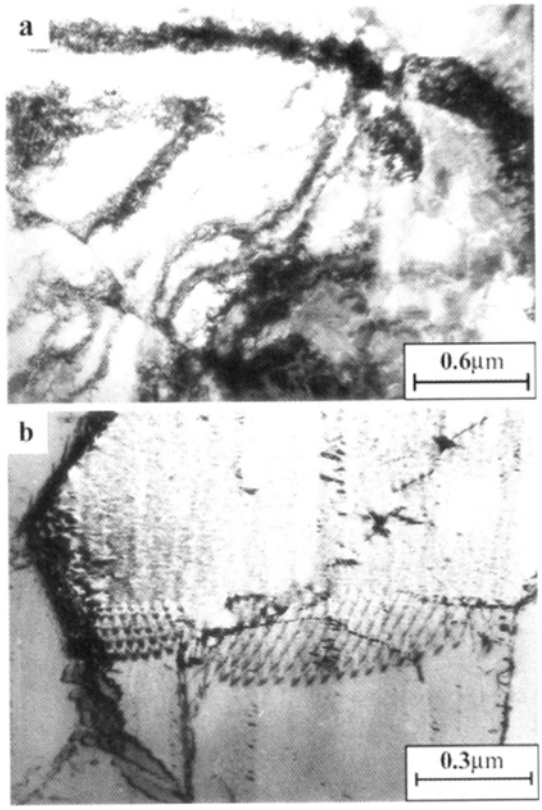

Fig. 11. TEM micrographs of the materials rolled at (a) 1373 K and (b) 1523 K (water quenched).

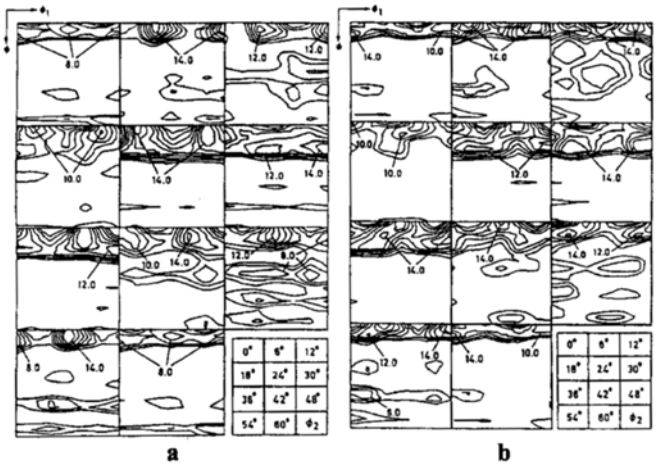

Fig. 12. ODFs for the Ti-24Al-11Nb alloy prior heat treated and rolled at 1173K to the thickness reductions (a) 50% and (b) 80%.

(Fig. 12). SEM micrograph of the 80% rolled material is shown in Fig. 13.

After examining the conditions for the development of a satisfactory basal texture, attention was focussed on its stability during further heat treatments that are usually undertaken for microstructural control. For this purpose, the material obtained by rolling of the prior heat treated alloy,

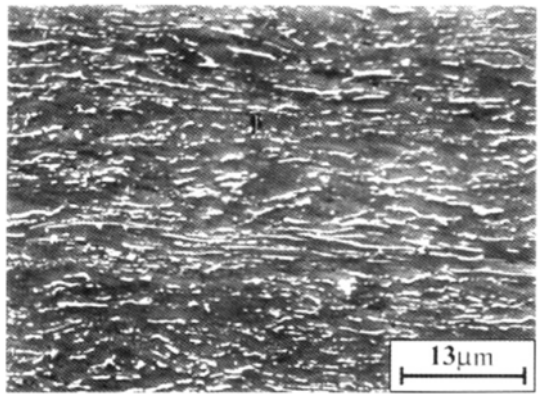

Fig. 13. SEM micrograph of the material prior heat treated and rolled at 1173 K for 80% rolling reduction.

which also exhibited a strong basal texture, has been subjected to isochronal annealing for 1 hr at temperatures 1123 K, 1173 K, 1233 K and 1293 K and then water quenched.

The above temperatures were chosen such that α_2 remains the major phase, thus allowing the effect of heat treatment on the basal texture of α_2 phase to be examined. It was observed that upon annealing at the lowest temperature, 1123 K, where recrystallisation of the α_2 just begins, the basal texture weakens perceptibly and a number of other non basal orientations develop. However it more or less regains its strength on annealing at 1173 K and 1233 K (Fig. 14). The basal texture again starts degrading at 1293 K. On the basis of the above results, further isothermal annealing was performed at 1173 K over intervals of time ranging between 15 min-12 hrs. The isothermally annealed samples also have shown initially a tendency for degradation of basal texture and evolution of non basal components for shorter annealing times, for instance 15 min, and re-intensification of the basal texture after relatively longer annealing times (Figs. 15(a)-(d)). However, a relatively prolonged annealing for 12 hrs was found to be deleterious for the basal texture. TEM microstructure of the materials annealed for 30 min and 2 hrs are shown in Figs. 16(a) and (b). As revealed from these

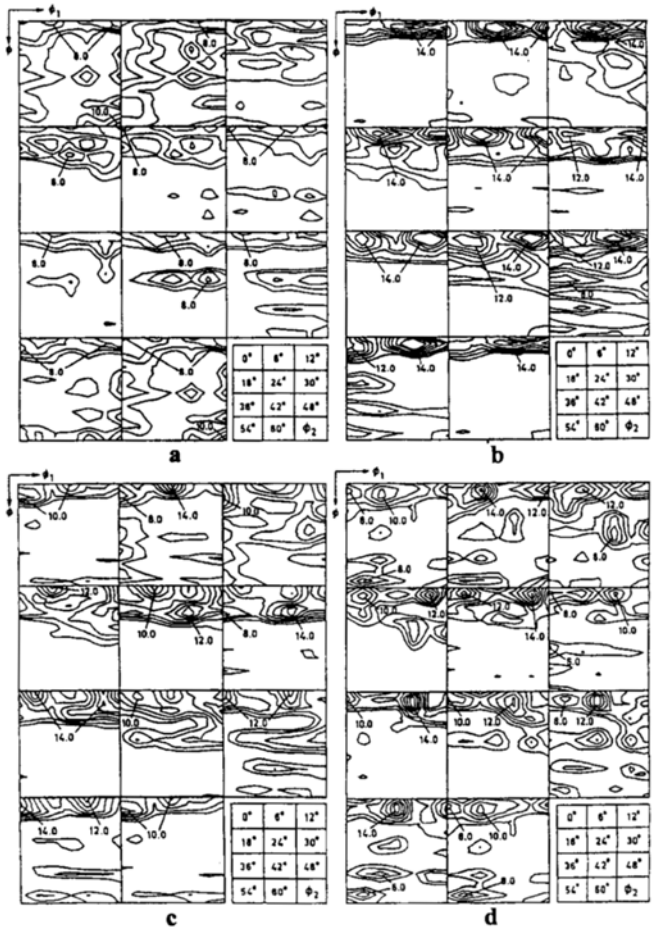

Fig. 14. ODFs of the Ti-24Al-11Nb alloy isochronally annealed for 1 hr at (a) 1123 K, (b) 1173 K, (c) 1233 K, (d) 1293 K.

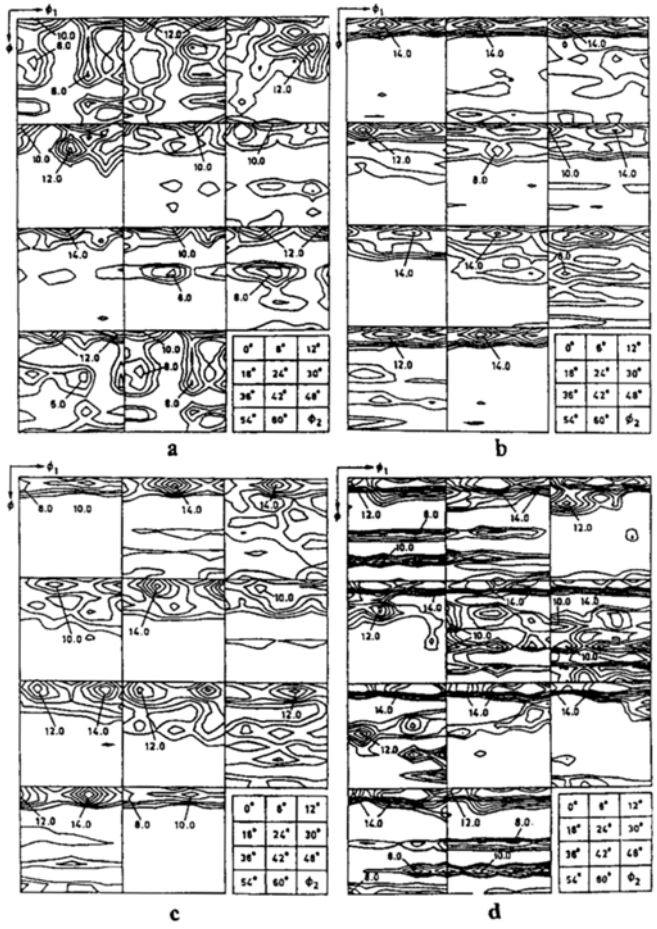

Fig. 15. ODFs of the Ti-24Al-11Nb alloy isothermally annealed at 1173 K for (a) 15 min, (b) 30 min, (c) 2 hrs and (d) 12 hrs.

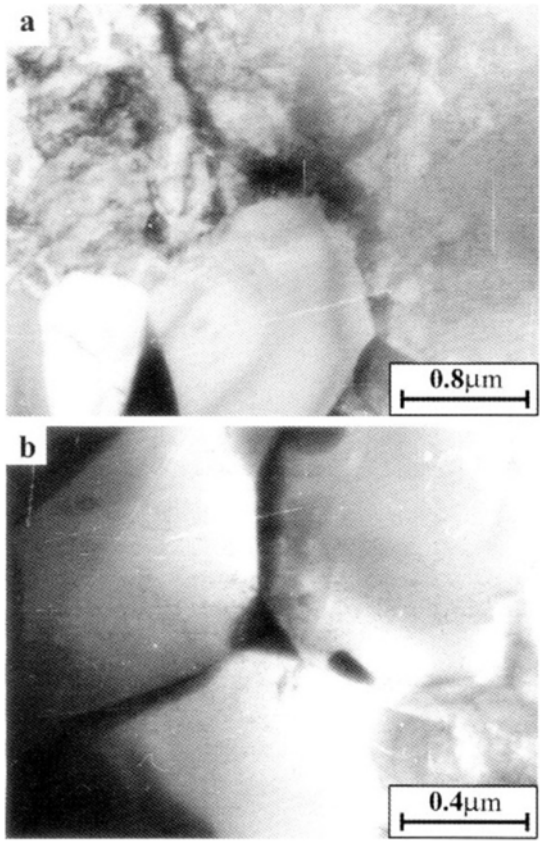

Fig. 16. TEM micrographs of the materials heat treated at 1173 K for (a) 15 min and (b) 2 hrs.

micrographs, the specimen annealed for 30 min shows highly recovered regions in addition to some recrystallised grains, whereas the 2 hrs annealed sample shows a more or less recrystallised microstructure. The similarity between the texture of these two materials further points to the fact that textural changes in the 15 min annealed sample are not exclusively due to recovery, and therefore may be associated with some changes in order. The above observations on textural changes on isochronal as well as isothermal annealing are compatible with the common behaviour of annealing textures of h.c.p. metals and alloys where the rolling textures are retained after recrystallisation. The degradation of rolling texture in the initial stages of annealing has been stipulated to be associated with some changes in the state of order of the α_2 phase. This is in conformity with the annealing behaviour of other aluminide intermetallics, such as Ni_3Al. It thus appears that rolling at lower temperatures with high amounts of reduction usually favours the development of basal texture which remains reasonably stable even after complete recrystallisation on heat treatment.

4. SUMMARY

Evolution of texture during processing of the aluminide intermetallics based on two-phase Ni_3Al and Ti_3Al has been thoroughly studied with the emphasis on understanding of the texture development during rolling as well as subsequent annealing. The study reveals some typical behaviour of these materials. For example, the Ni_3Al base alloy exhibits strain induced texture transformation (from pure metal to alloy type), which is accompanied by a change in the state of order of the material (from $L1_2$ to DO_{22} structure). Annealing produces a drastic weakening of the sharp deformation texture, right after the recovery stage finally producing a texture not far from the random. On the other hand, the basal texture is developed in Ti_3Al-Nb alloy during thermomechanical processing with suitable choice of processing variables. Processing in the near α_2 phase field enhances the intensity of basal texture. Annealing of the as-rolled material causes perceptible weakening of basal texture during the recovery stage, which however intensifies as annealing proceeds. The basal texture appears to remain rather stable during the recrystallisation process, which does not involve any phase transformation.

REFERENCES

1. C. T. Liu and K. S. Kumar, *J. Metals* **45**, 38 (1993).
2. C. T. Liu, J. O. Steigler, and F. H. Froes, *Metals Handbook*, 10th ed., vol. 2, p.913, ASM International, Metals Park, OH (1990).
3. K. Aoki and O. Izumi, *J. Jpn. Inst. Met.* **43**, 1190 (1977).
4. V. K. Sikka, *MRS Symp. Proc.* **133**, 487 (1989).
5. A. Choudhury, A. K. Mukherjee and V. K. Sikka, *J. Mater. Sci.* **25**, 3142 (1990).
6. M. S. Kim, S. Hanada, S. Watanabe and O. Izumi, *Trans. JIM* **30**, 77 (1989).
7. R. Z. Valiv, R. M. Gayanow, H. S. Yang and A. K. Mukherjee, *Scripta metall. mater.* **25**, 1945 (1991).
8. B. Bhattacharya, *Ph. D. Thesis*, I. I. T. Kanpur (1996).
9. S. Ghosh Chowdhury, *Ph. D. Thesis*, I. I. T. Kanpur (1995).
10. S. Ghosh Chowdhury, R. K. Ray and A. K. Jena, *Scripta metall. mater.* **32**, 1501 (1995).
11. J. Hirsch, K. Lücke and M. Hatherly, *Acta metall.* **36**, 2863 (1988).
12. B. J. Duggan, M. Hatherly, W. B. Hutchinson, and P. T. Wakefield, *Metal Sci.* **12**, 343 (1978).
13. W. B. Hutchinson, F. M. C. Besag, and C. V. Honess, *Acta metall.* **21**, 1685 (1973).
14. J. Ball and G. Gottstein, *Intermetallics* **1**, 171 (1993).
15. J. Ball and G. Gottstein, *Intermetallics* **1**, 191 (1993).
16. J. Ball and G. Gottstein, *Intermetallics* **2**, 205 (1994).

17. J. Ball, B. Zeumer and G. Gottstein, *Intermetallics* **3**, 209 (1995).
18. G. Gottstein, P. Nagpal and W. Kim, *Mater. Sci. Eng.* **A 108**, 165 (1989).
19. C. Escher, S. Neves and G. Gottstein, *Acta mater.* **46**, 441 (1998).
20. G. Wassermann, *Z. Metallkde.* **54**, 61 (1963).
21. S. Ghosh Chowdhury, R. K. Ray and A. K. Jena, *Mater. Sci. Eng.* **A 246**, 289 (1998).
22. R. K. Ray, B. Bhattacharya and S. Ghosh Chowdhury, *Textures of Materials-Proc. of ICOTOM-11* (eds., Z. Liang, L. Zuo, Y. Chu), p. 336, International Academic Publishers, Beijing, Xian, China (1996).
23. S. Ghosh Chowdhury, R. K. Ray and A. K. Jena, *J. Mater. Sci. Lett.* **15**, 1710 (1996) .
24. J. Kumpfert and C. H. Ward, *Advanced Aerospace Materials* (ed., H. Buhl), p. 73, Materials Research and Engineering, Springer-Verlag, New York (1993).
25. M. J. Blackburn and M. P. Smith, *Research to Conduct an Exploratory and Analytical Investigation of Alloys*, AFML-TR-78-18 (1978).
26. D. Banerjee, *Intermetallic Compounds: Vol. 2, Practice* (eds., J. H. Westbrook, and R. L. Fleischer), p. 91, John Wiley & Sons Ltd., New York (1994).
27. H. A. Lipsitt, *Advanced High Temperature Alloys: Processing and Properties* (eds., S. M. Allen, R. M. Pelloux and R. Widmer), p. 157, ASM International, Metals Park, Ohio (1986).
28. W. P. Hon, C. H. Koo, S. K. Wu and T. S. Chou, *Scripta metall.* **25**, 2171 (1991).
29. D. B. Knorr and N. S. Stoloff, *Mater. Sci. Eng.* **A 123**, 81 (1991).
30. S. F. Frederick and G. A. Lenning, *Metall. Trans.* **6 B**, 601 (1975).
31. Satyam Suwas, *Ph. D. Thesis*, I. I. T. Kanpur (1998).